Performance Optimization in ROADM-Enabled DWDM Systems Using Flexible Modulation Formats

Wei Wang[1], Qunbi Zhuge[1,2], Yuliang Gao[1,3], Xian Xu[1], and David V. Plant[1]
[1]*Department of Electrical and Computer Engineering, McGill University, Montreal, QC, H3A 2A7, Canada*
[2]*Ciena Corporation, Ottawa, Ontario, Canada, K2H 8E9*
[3]*Photonics Research Centre, Department of Electrical Engineering, The Hong Kong Polytechnic University, Hong Kong*
wei.wang15@mail.mcgill.ca

Abstract: The time domain hybrid QAM enabled flexible transceiver is proposed to adaptively optimize the transmission performance in DWDM systems with cascaded ROADMs. Comprehensive performance investigations are conducted for both fixed and flexible grid systems.
OCIS codes: (060.1660) Coherent communications; (060.2330) Fiber optics communication

1. Introduction

With the 100G and 200G coherent optical transceivers being commercialized, next generation transceiver is expected to deliver a signal bandwidth larger than 50 GHz to support 400G transmissions. Moreover, flexible transceivers with reconfigurable bandwidth and spectral efficiencies (SE) are also exploited for future agile optical networks [1,2]. In the meantime, the dense wavelength division multiplexing (DWDM) infrastructure is also being revolutionized from fixed 50 GHz grid to flexible grid with a spacing granularity of 12.5 GHz [3]. The reconfigurable optical add and drop multiplexers (ROADM) using wavelength selective switches (WSS) are the key elements for current and future dynamic optical networks [4]. However, the narrow filtering effects from cascaded ROADMs limit the available bandwidth for each WDM channel and the current optical transceiver is normally designed to tolerate the worst case [4].

Recently, we proposed the use of the time domain hybrid QAM (TDHQ) technique to realize a continuous tuning of the system SE and transmission distance for flexible transceivers [5]. In this work, we investigate the adaptive performance optimization using the TDHQ-enabled flexible transceiver for the links with different filtering and bandwidth conditions. Other techniques including root M-shaped pulse (RMP) shaping [6], root polynomial pulse (RPP) shaping [7], and duobinary modulation scheme [8,9] are also examined for comparisons. We first propose a universal digital signal processing (DSP) platform to ensure that system performances are independent of the receiver processing algorithms, and that all the systems have similar implementation complexities for fair comparison. Then by simulation we compare system performances for both 100G and 200G systems on the legacy fixed 50-GHz grid. In addition, the performances for future 400G system on the flex-grid are compared considering the filtering effects from cascaded WSSs. A significant overall performance improvement is demonstrated by adaptively optimizing the signal bandwidth and SE using the TDHQ-enabled flexible transceivers.

2. System setup and DSP procedure

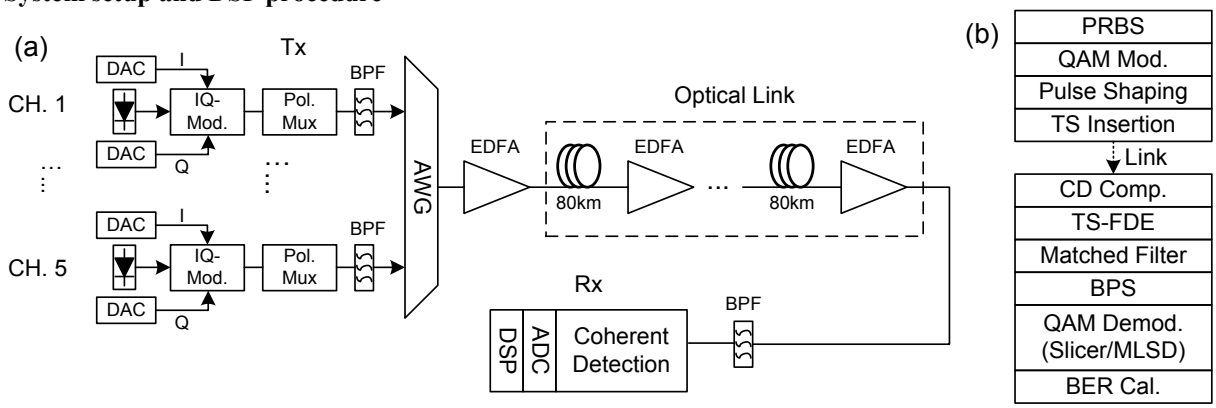

Fig. 1. (a) Simulation setup; (b) Main transmitter and receiver DSP diagram. Tx: Transmitter. Rx: Receiver. CH.: Channel. IQ-Mod.: In phase and quadrature modulator. Pol. Mux: Polarization multiplexer. BPF: Band pass filter. ADC: Analog-to-digital convertor. PRBS: Pseudo-random binary sequence. Mod. : Modulation. CD: Chromatic dispersion. FDE: Frequency domain equalization. Cal.: Calculation.

Fig. 1(a) shows the simulation setup. At the transmitter (Tx), the processed waveform was sent to the digital-to-analog converters (DAC) followed by the optical IQ modulation and polarization division multiplexing (PDM). Then the optical signal was passed through a 5th order Gaussian filter to confine the total bandwidth. Five uncorrelated WDM channels were combined by an arrayed waveguide grating (AWG), amplified and then launched

into an optical link with each span containing 80 km standard single mode fiber (SSMF) and an Erbium doped fiber amplifier (EDFA) with 5dB noise figure. At the receiver (Rx), the central channel was filtered, coherently detected, and digitally processed.

Fig. 1(b) shows the proposed main transmitter and receiver DSP. With the aid of training symbol (TS) enabled single carrier frequency domain equalization (SC-FDE), the pre-/post- filter and the multi-modulus equalization module for equalizing duobinary systems in [8,9] are no longer needed, and the complexity is significantly reduced [10]. Carrier phase is recovered using the blind phase search (BPS) algorithm, which does not require duobinary symbols to be transferred to QAM symbols first [11]. The aforementioned two processing techniques are universal for all the systems considered in this work. For duobinary systems, a trellis structured maximum likelihood sequence detection (MLSD) is used for symbol demodulation, whereas for other systems a simple slicer is used for symbol decision. As a reference, the widely adopted RRC system is also included for comparison. Table 1 summarizes all the system specifications in our simulations.

Table 1. System specifications

system type	RRC/RMP/RPP				TDHQ				Duobinary	
bit rate (raw bit rate)-Gb/s	100 (112)	200 (250)	400 (500)		100 (112)	200 (250)	400 (500)		400 (500)	
grid (signal bandwidth)-GHz	50 (40)	50 (40)	62.5 (65)	75 (65)	50 (40)	50 (40)	62.5 (62.5)	75 (65)	62.5 (62.5)	75 (62.5)
modulation format (ratio)	QPSK	16QAM	16QAM	16QAM	B/QPSK(1/1)	8/16QAM(3/1)	Optimized	Optimized	16QAM	16QAM
baud rate-Gbaud	28	31.25	62.5	62.5	38	38.5	Optimized	Optimized	16QAM	16QAM
overhead (FEC/Protocol)-%	12 (7/5)	25 (20/5)	25 (20/5)	25 (20/5)	12 (7/5)	25 (20/5)	25 (20/5)	25 (20/5)	25 (20/5)	25 (20/5)

3. 100G and 200G system results

For the traditional 50 GHz grid, we assume a 10 GHz guard band to prevent the inter-carrier cross talk between neighbouring channels and inter-symbol interference (ISI) caused by ROADMs. 100G RRC, RMP, RPP, and TDHQ signals are considered with the system parameters listed in Table 1. Fig. 2(a) and 2(b) show the system back to back (B2B) and the transmission performance for 100G transmissions, respectively. The four systems have similar OSNR requirement in the linear region. However, in the nonlinear region, the transmission distances of RMP and RPP are extended by 120 (2%) and 180 (3%) km compared to RRC, respectively, because of the reduced intra-channel nonlinearity using a 40 GHz spectrum to transmit 28 Gbaud signals [6,7]. The TDHQ signal is composed of 1/1 BPSK/QPSK at 38 Gbaud. It can be seen that the nonlinear noise is reduced significantly as shown in Fig. 2(b) at high launch powers. This is because the same power is evenly distributed to a wider range of frequencies leading to a stronger phase mismatch in the nonlinear interaction, and lower order QAM (in this case, BPSK) has a higher nonlinear tolerance. At the optimum launch power, the transmission distance of TDHQ is extended by 320 (5.3%) km compared to RRC.

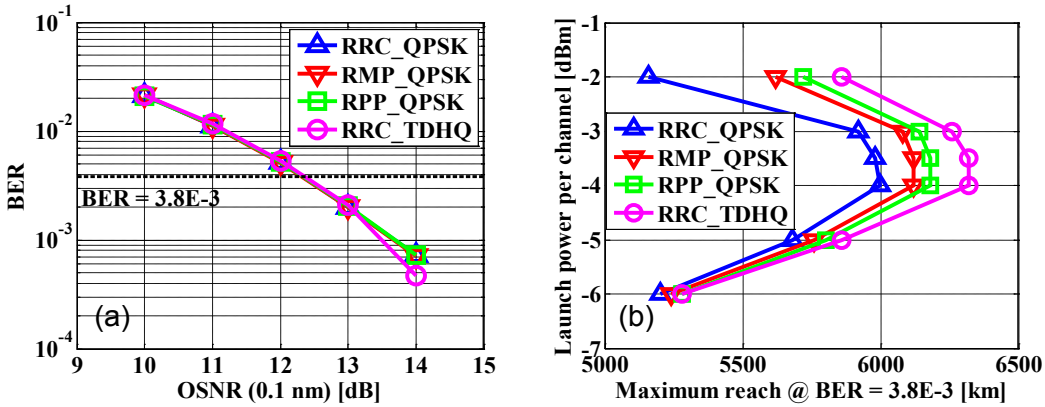

Fig. 2. 100G system performances: (a) back to back BER vs. OSNR; (b) launch power per channel vs. maximum reach @ BER = 3.8E-3

For a 200G (raw 250 Gb/s) system on the fixed 50 GHz grid with a 10 GHz guard band, 8QAM doesn't satisfy the SE requirement. Therefore, 16QAM at 31.25 Gbaud is considered here. For TDHQ, the 200G system is realized at 38.5 Gbaud by mixing the 8QAM and 16QAM at the ratio of 3:1 as shown in Table 1. Fig. 3(a) and 3(b) show the B2B and the transmission performance, respectively. Due to the reduced roll-off factor and the increased signal baud rate, RMP and RPP don't improve the performance with respect to the RRC system [6]. On the other hand, due to the large portion of 8QAM symbols, TDHQ requires ~1 dB less OSNR at the BER threshold in the B2B situation. Together with the increased nonlinear tolerance as explained earlier, the TDHQ system achieves 740 km (30%) longer maximum distance than the rests for 200G transmissions.

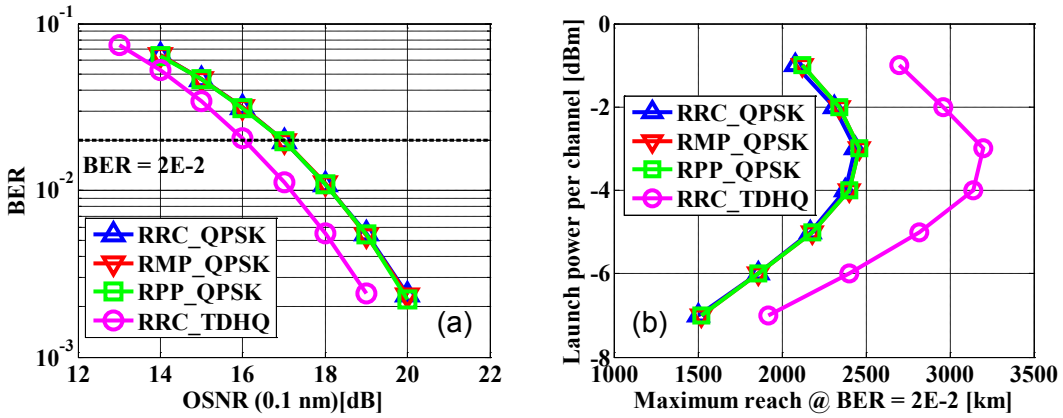

Fig. 3. 200G system performances: (a) back to back BER vs. OSNR (0.1nm); (b) launch power per channel vs. maximum reach @ BER = 2E-2

4. 400 G system results

For future 400G (raw 500 Gb/s) systems, we consider two flex-grid scenarios including 62.5 GHz and 75 GHz grid. The filtering effects from cascaded WSSs were included, where the WSS were simulated based on the model in [12]. The inset (1) of Fig. 4(a) shows the simulation setup, where the noise is loaded after each WSS in a distributive manner. Fig. 4(a) shows the cascaded WSS effects, where the 3 dB bandwidth is reduced by up to 10 GHz after passing 30 WSSs. In such stringent bandwidth requirement, we compare the performance of RRC-16QAM, TDHQ and duobinary system, which all satisfy the high SE requirement.

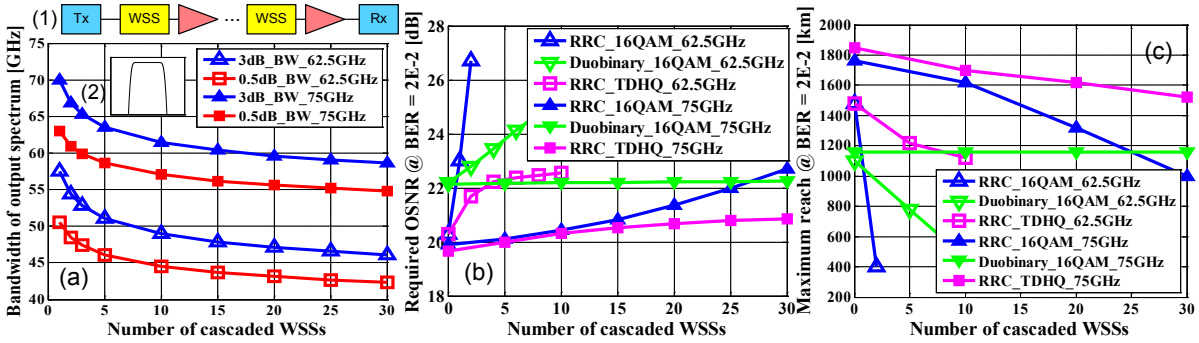

Fig. 4. 400G system performances for 62.5GHz and 75GHz grid. (a) effects of cascaded WSS on the output bandwidth. Insets: (1) simulation model; (2) WSS model; (b) back to back performance; (b) transmission performance

Fig. 4(b) and 4(c) show the B2B and transmission performance, respectively. The performance of TDHQ is dynamically optimized by tuning the SE according to the available bandwidth for each cascaded WSSs case to avoid the ISI. It is shown that the RRC 16QAM has the worst tolerance to the ISI while duobinary and TDHQ are both quite tolerant to the filtering effects. However, there is about 2 dB innate penalty of duobinary system from violating the ISI free Nyquist criterion compared with the Nyquist systems of the same SE [8]. With the dynamically optimized SE, TDHQ shows a reduced required OSNR at the BER threshold compared to duobinary system and a much better cascaded WSSs tolerance compared to the RRC 16QAM for both channel spacing cases.

4. Conclusion

We demonstrated that the performance of DWDM systems with cascaded ROADMs can be adaptively optimized with the TDHQ-enabled flexible transceivers, and an overall significant improvement can be achieved for various system requirements and link conditions.

5. References

[1] Q. Zhuge, et al., Opt. Exp., **22**, 2278-2288 (2014).
[2] K. Roberts, et al., ECOC'12, We.3.A.3 (2012).
[3] ITU-T recommendation G.694.1.
[4] Y. Hsueh, et al., JLT, **30**, 3980-3986 (2012).
[5] Q. Zhuge, et al., JLT, **25**, 2621-2628 (2013).
[6] X. Xu, et al., Opt. Exp., **21**, 31966-31982 (2013).
[7] A. S. Karar, et al., OFC'14, Tu3A.7 (2014).
[8] J. Li, et al., JLT, **30**, 1664-1676 (2012).
[9] J. Zhang, et al., JLT, **32**, 3239-3246 (2014).
[10] D. Falconer, et al., Communications Magazine, **40**, 58-66 (2002).
[11] T. Pfau, et al., JLT, **27**, 989-999 (2009).
[12] C. Pulikkaseril, et al., Opt. Exp., **19**, 8458-8470 (2011).